

GHRIS Instrument Overview

In This Chapter...

GHRIS History / 34-2
Instrument Description / 34-3
Operating Modes and Data Types / 34-11
Documentation and References / 34-12

The Goddard High Resolution Spectrograph (GHRIS) was designed by the GHRIS Investigation Definition Team (IDT) consisting of J. Brandt (Principal Investigator), E. Beaver, A. Boggess, K. Carpenter, D. Ebbets, S. Heap, J. Hutchings, M. Jura, D. Leckrone, J. Linsky, S. Maran, B. Savage, A. Smith, L. Trafton, F. Walter, and R. Weymann. The instrument was built by Goddard Space Flight Center and prime subcontractor Ball Aerospace. The instrument is described in Brandt, J.C., et al., 1994, “The Goddard High Resolution Spectrograph: Instrument, Goals, and Science Results,” *PASP*, 106, 890.

You are probably someone who wishes to study archival data from the GHRIS since most General Observers (GOs) have completed their data analysis by now. Archival Researchers (ARs) face several problems—only some of which the original observer experienced:

- Determining if any GHRIS observations in the archive are likely to be useful for your purposes. To understand the basic properties of the GHRIS, you may wish to refer to the *GHRIS Instrument Handbook* version 6 because that document was written to guide people writing the detailed proposals that led to the observations that are in the archive. This *HST Data Handbook* includes many portions of the instrument handbook that are useful for archival research.
- Retrieving appropriate observations and other data files needed to calibrate them. Data retrieval and the use of StarView are discussed in Chapter 1 (Volume 1).

- Understanding how those observations were planned and obtained, and assessing overall data quality. Again, the *GHRIS Instrument Handbook* best explains how and why observations were taken, although most archival users will find this handbook sufficient. Data assessment for the GHRIS is discussed in Chapter 35.
- Recalibrating those observations using the best available knowledge of the instrument. This is the major focus of this handbook.
- Analyzing the observations to extract useful observational quantities. Most of the discussion here is on data reduction, but some aspects of analysis are covered as well.

Of course data reduction is what you must do before you get to the interesting work, which is extracting useful astrophysical information from your data. Reading manuals about the data reduction process is seldom more entertaining than the reduction itself. Our goal in this handbook is to save you a lot of wasted time and effort by helping you to do the reduction job right the first time.

This section follows the basic outline of all of the chapters of this handbook. This first GHRIS chapter (Chapter 34) describes the instrument, its general use, and important sources of additional information. Chapter 35 describes the data formats and data assessment—methods for determining whether the target was successfully acquired and the overall quality of the data. Chapter 36 describes the calibration process and how results can be improved. Chapter 37 describes error sources and uncertainty—topics intertwined with calibration. Chapter 38 concludes the GHRIS part of this manual and describes various topics related to data analysis.

Although the GHRIS was retired as an active instrument, STScI continues to provide analysis support for GHRIS data. GHRIS questions should be sent via E-mail to: help@stsci.edu. Any updates to GHRIS documentation and calibration will be summarized in the HST Spectrographs Space Telescope Analysis Newsletter (STAN).

34.1 GHRIS History

Critical events in the operational history of the GHRIS include:

1. The GHRIS was launched inside HST in April 1990.
2. The Side 1 low-voltage power supply (LVPS) had repeated problems in the summer of 1991, eliminating access to both low- and high-dispersion modes in the far-UV (G140L and Ech-A). Prior to this loss, Ech-A was the most-requested GHRIS grating, but deconvolution techniques allowed G160M observations to approach Ech-A resolution. Hence some of this science was done with Side 2 during Cycles 2 and 3.

3. The LVPS problem was fixed during the first servicing mission, restoring important capabilities and leading to greater GHRS usage.
4. The failure of the SC1 calibration lamp eliminated redundancy for wavelength calibration. Fortunately, the specifications for lamps were very conservative and SC2 had ample lifetime to meet observer needs.
5. Acquisitions during the early years had to specify BRIGHT and FAINT limits, leading to failed acquisitions and wasted telescope time. Implementation of BRIGHT=RETURN eliminated this problem. Also, BRIGHT=RETURN used 32 bits, preventing register overflow.
6. Corrective Optics Space Telescope Axial Replacement (COSTAR), installed during the first servicing mission of December 1993, changed the net throughput of the large science aperture (LSA) by very little (two extra reflections offset the better PSF), but the contrast of the PSF changed enormously, resulting in reliable fluxes. Small science aperture (SSA) throughput improved too, by about a factor of two.
7. Before COSTAR, HST's spherical aberration was sometimes a "feature" for acquisitions in the sense that the algorithm could find the wings of the PSF even when centering was poor.
8. A catastrophic failure occurred one week before the second servicing mission, resulting in the complete shutdown of the GHRS. The most important loss was some special observations that were to be made with the COSTAR mirrors withdrawn to try to determine the origin of far-UV sensitivity losses.

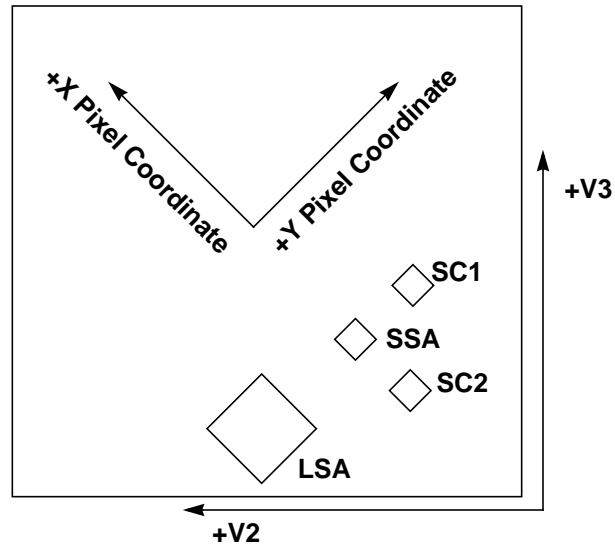
34.2 Instrument Description

The GHRS was one of the first-generation science instruments aboard HST. The spectrograph was designed to provide a variety of spectral resolutions, high photometric precision, and excellent sensitivity in the wavelength range 1100 to 3200 Å. The GHRS was a modified Czerny-Turner spectrograph with two science apertures (large: LSA, and small: SSA), two detectors (D1 and D2), several dispersers, and camera mirrors. There were also a wavelength calibration lamp, flatfield lamps, and mirrors to acquire and center objects in the observing apertures.

Schematics of the mechanical and optical layout are shown below and can be found in the *GHRS Instrument Handbook*, 6.0, Figures 6-1 to 6-9. The GHRS was installed as one of the axial scientific instruments, with the entrance aperture adjacent to FGS 2 and FGS 3. With the installation of COSTAR, the entrance apertures were at the former position of the High Speed Photometer. The GHRS had two science apertures, designated Large Science Aperture (LSA or 2.0) and Small Science Aperture (SSA or 0.25). The 2.0 and 0.25 designations were the pre-COSTAR size of the apertures in arcseconds. The post-COSTAR size of the LSA was 1.74 arcsec square and the SSA was 0.22 arcsec square. The separation of the two apertures was approximately 3.7 arcsec on the sky and 1.05 mm on the

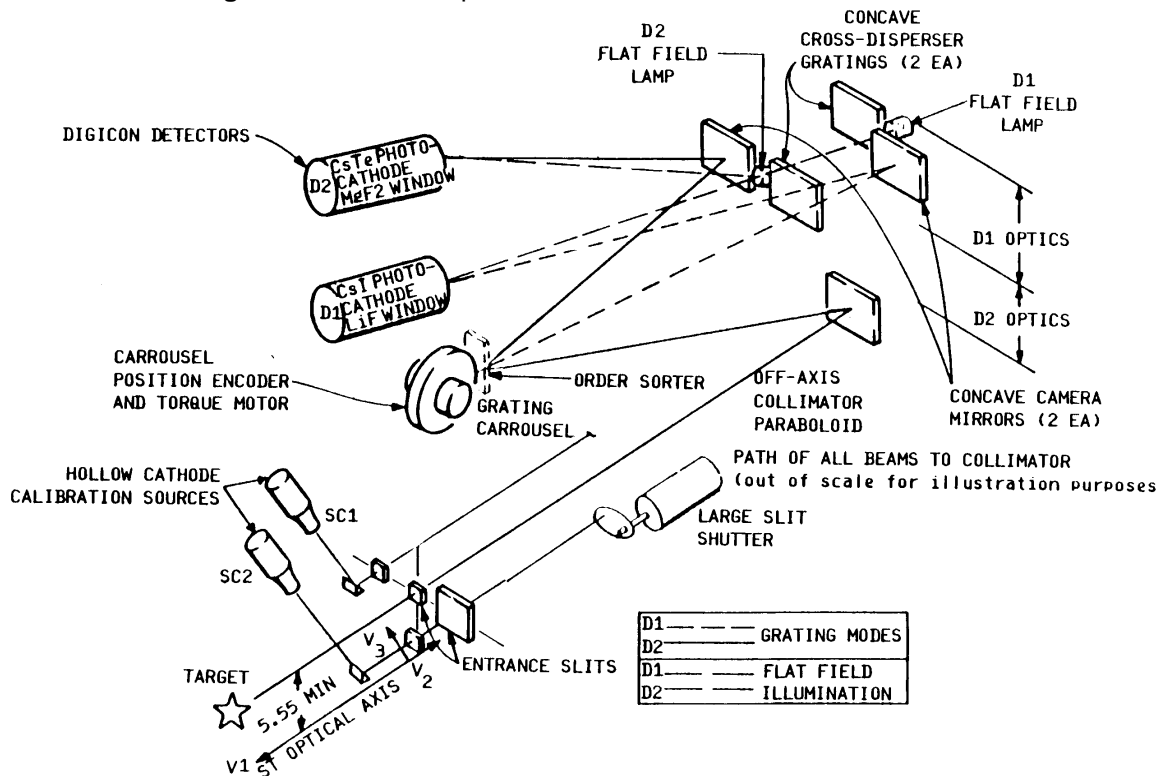
slit plate. The LSA had a shutter to block light from entering the spectrograph when the SSA was being used, while the SSA was always open. Because of this, scattered light from a bright target in the SSA could contaminate a wavelength calibration exposure (*wavecal*). The locations of the GHRIS apertures relative to the spacecraft axes are displayed in Figure 34.1.

Figure 34.1: Aperture Locations Relative to Spacecraft Axes



Light from a target was collected by HST and focused onto one of the two GHRIS apertures. After passing through an aperture, the light struck the collimating mirror and was directed toward the grating carousel. The collimated beam illuminates one of the gratings or a flat mirror; selection of a grating or mirror was performed by rotating the carousel. Camera mirrors focused the dispersed light onto one of the Digicon photocathodes. Photoelectrons from the Digicons were focused onto a linear silicon diode array.

Figure 34.2: GHRS Optics



34.2.1 Dispersers

The dispersers were mounted on a rotating carousel, together with several plane mirrors used for acquisition. The first-order gratings were designated as G140L, G140M, G160M, G200M, and G270M, where “G” indicates a grating, the number indicates the blaze wavelength (in nm), and the “L” or “M” suffix denotes a “low” or “medium” resolution grating, respectively. The GHRS medium resolution first-order gratings were holographic in order to achieve very high efficiency within a limited wavelength region. G140L is a ruled grating.

Side 1 first-order gratings, G140L and G140M, had their spectra imaged by mirror Cam-A onto detector D1, which had a cesium iodide photocathode and was best for the shortest wavelengths (about 1050 to 1700 Å). The other three (Side 2) gratings had their spectra imaged by Cam-B onto detector D2, which had a cesium telluride photocathode and worked best at wavelengths from about 1700 to 3200 Å, but which was also useful down to 1200 Å. Also note that detector D2 had a MgF₂ front plate, which attenuated severely below Lyman-α, but that detector D1 had a LiF faceplate for better throughput at the shortest wavelengths. Note that little or no flux below 1150 Å was reflected by the COSTAR mirrors because of their magnesium fluoride coatings. Figure 34.3 shows the GHRS acquisition optics; the main acquisition mirror is N2. The useful spectral wavelength ranges of the first order gratings are listed in Table 34.1.

Figure 34.3: GHR Acquisition Optics

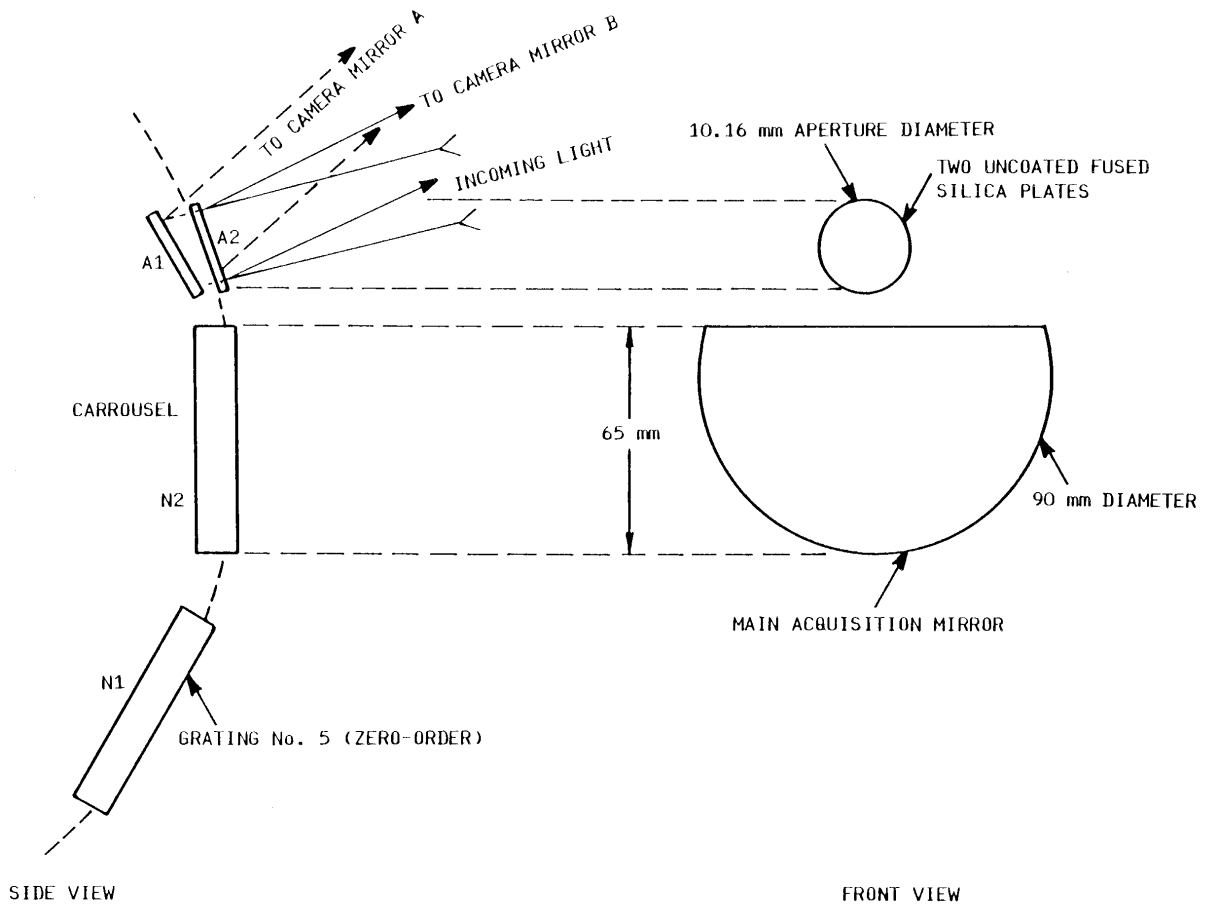


Table 34.1: Useful Wavelength Ranges for First-Order and Echelle Gratings

Grating	Useful Range (Å)	Å per diode	Bandpass (Å)	Comment
G140L	1100–1900	0.572–0.573	286–287	
G140M	1100–1900	0.056–0.052	28–26	
G160M	1150–2300	0.072–0.066	36–33	2nd order overlap above 2300 Å
G200M	1600–2300	0.081–0.075	41–38	2nd order overlap above 2300 Å
G270M	2000–3300	0.096–0.087	48–44	2nd order overlap above 3300 Å
Echelle A	1100–1700	0.011–0.018	5.5–9	
Echelle B	1700–3200	0.017–0.034	8.5–17	

The carrousel also had an echelle grating. The higher orders were designated as mode Ech-A, and they were imaged onto D1 by the cross-disperser CD1. The lower orders were designated as mode Ech-B, and they were directed to D2 by

CD2. The useful spectral range of the echelle gratings are provided in Table 34.1. Only a single order was recorded in a single observation.

Finally, mirrors N1 and A1 imaged the apertures onto detector D1, and mirrors N2 and A2 imaged onto D2. The “N” mirrors are “normal,” i.e., unattenuated, while the “A” mirrors (“attenuated”) reflect a smaller fraction of the light to the detectors, so as to enable the acquisition of bright stars. (The mode designated as N1 actually used the zero-order image produced by grating G140L.)

Bright targets were acquired with one of the attenuated mirrors, A1 or A2. These acquisitions took substantially longer than if the N1 or N2 mirrors were used. SSA acquisitions (ACQ/PEAKUPs) with the A1 mirror were usually doubled up to center the target in the SSA. Acquiring a target in the SSA first requires a LSA acquisition (3 x 3 search) followed by a SSA acquisition (5 x 5 search).

The GHRS LSA was 74 arcseconds from the FOS Blue aperture. Starting with Cycle 5, it became possible to acquire a faint target with the FOS and slew the telescope to position the target into the GHRS LSA. It also became possible to acquire a bright target with the GHRS and slew the telescope to position the target into the FOS Blue aperture. Therefore, a GHRS proposal executed during Cycles 5 and 6 may contain FOS observations (which you would have to request from the archive separately). This can be seen by examining the Phase II proposal.

34.2.2 Detectors

Use of the various gratings or mirrors produces one of three kinds of GHRS data:

- An image of the entrance aperture, which may be mapped to find and center the object of interest.
- A single-order spectrum.
- A cross-dispersed, two-dimensional echelle spectrum.

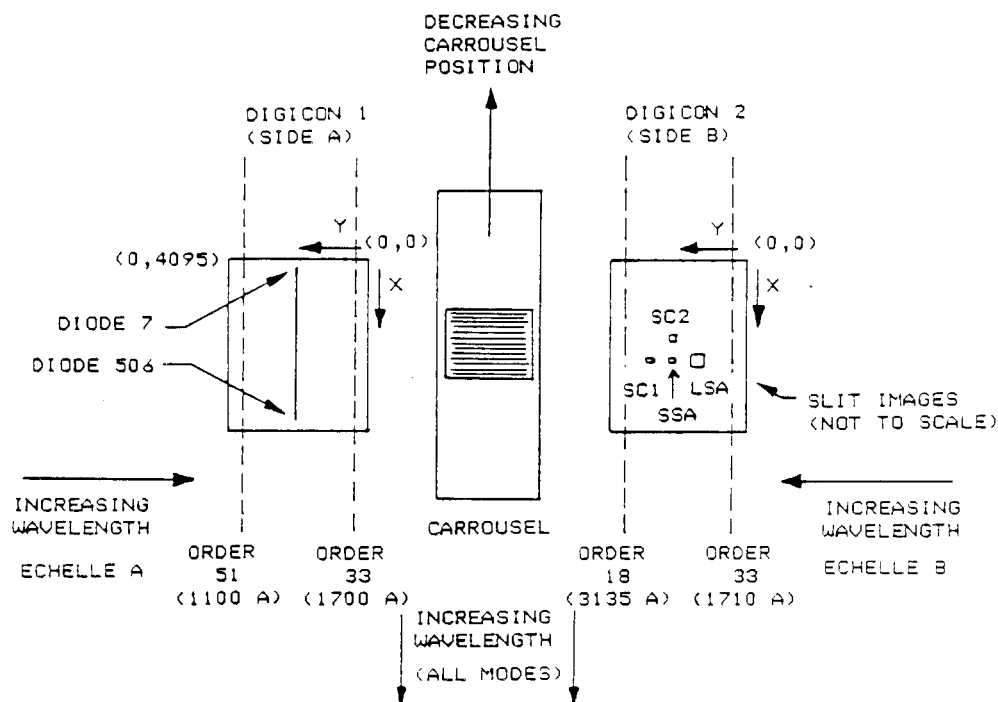
The flux in these images was measured by photon-counting Digicon detectors; the portion of the image plane that was mapped onto the Digicon is determined by magnetic deflection coils. These detectors were the heart of the GHRS and they involve subtleties that must be understood if data are to be reduced properly and competently.

The Detectors and Their Diodes

There were two Digicons: D1 (also known as Side 1) and D2 (Side 2). D1 had a cesium iodide photocathode on a lithium fluoride window that makes D1 effectively *solar-blind*, i.e., the enormous flux of visible-light photons that dominates the spectrum of most stars will produce no signal with this detector, and only far-ultraviolet photons (1060 to 1800 Å) produce electrons that are accelerated by the 23 kV field onto the diodes. D2 had a cesium telluride photocathode on a magnesium fluoride window. Each Digicon had 512 diodes that accumulated counts from accelerated electrons. 500 of those are *science diodes*, plus there are *corner diodes* and *focus diodes*.

The 500 science diodes were 40 x 400 microns on 50 micron centers. The focus diodes were 25 x 25 microns and there were three located on each end of the array. Two 1,000 x 100 micron diodes were used to measure background and two 1,000 x 100 micron diodes were used to monitor high energy protons. Eight diodes mapped the LSA and the SSA was 1 diode wide and 1/8 diode high.

Figure 34.4: View from the Cross-Dispersers toward the Digicon Detectors (illustrates senses of x and y motions and of increasing wavelength)



Photocathode Granularity and FP-SPLIT Observing

Both photocathodes had granularity—irregularities in response—of about 0.5% (rms) that could limit the S/N achieved, and there were localized blemishes that produced irregularities of several percent. The Side 1 photocathode also exhibited features called “sleeking,” which are slanted, scratch-like features that have an amplitude of 1 to 2% over regions as large as half the faceplate. The effects of these irregularities could, in principle, be removed by obtaining a flatfield measurement at every position on the photocathode, but that was generally impractical. Instead, the observing strategy was to rotate the carrousel slightly between separate exposures and so use different portions of the photocathode. This procedure is called an FP-SPLIT, and with it each exposure was divided into two or four separate-but-equal parts, with the carrousel moving the spectrum about 5.2 diode widths each time in the direction of dispersion. These individual spectra could be combined together during the reduction phase.

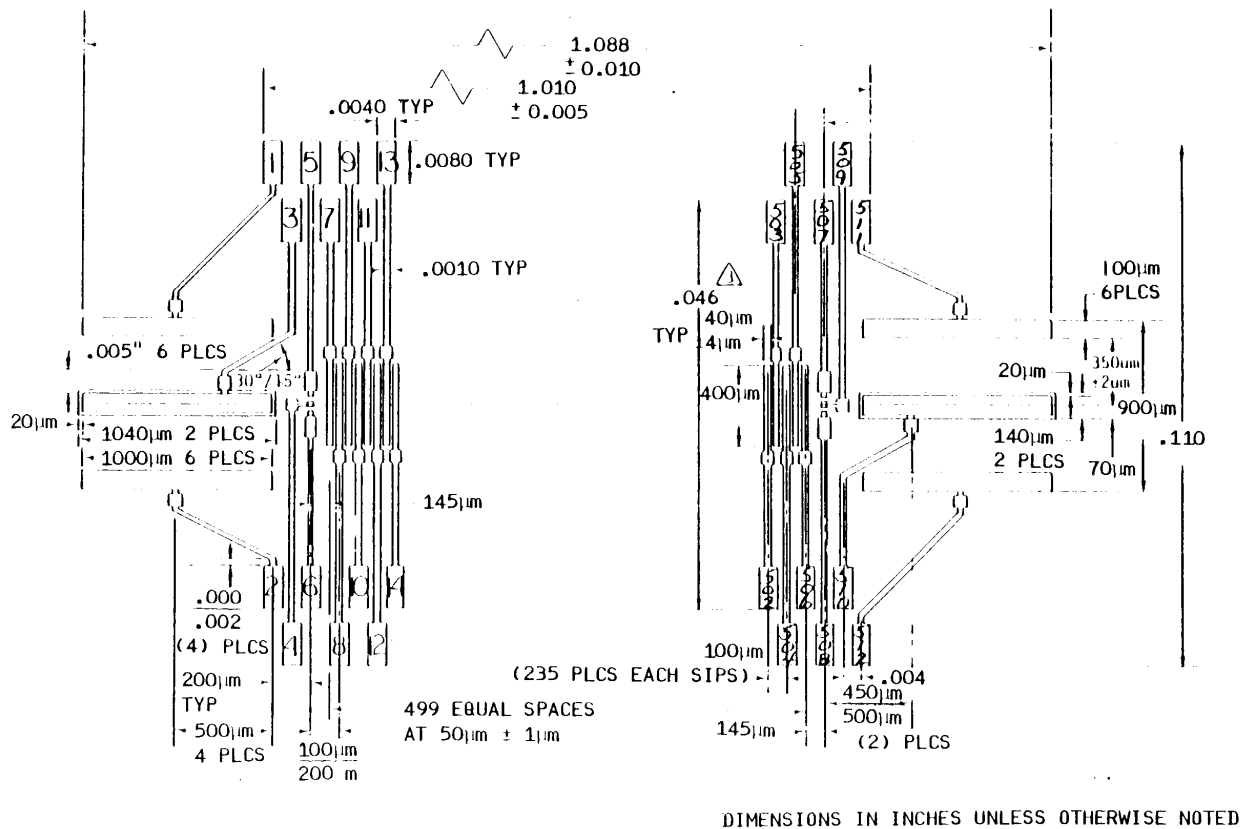
Diode Irregularities and the Use of Comb-Addition

The diodes in the Digicons also had response irregularities, but these were very slight. The biggest effect was a systematic offset of about 1% in response of the odd-numbered diodes relative to the even-numbered ones. This effect could be almost entirely defeated by use of the default COMB addition procedure. COMB addition deflected the spectrum by an integral number of diodes between subexposures and had the additional benefit of working around dead diodes in the instrument that would otherwise leave image defects.

Sampling and Substepping with STEP-PATT

The Digicons' diodes were about the same width as the FWHM of the point spread function (PSF) for HST. Thus the true resolution of the spectrum could not be realized unless it was adequately sampled. That was done by making the magnetic field move the spectrum by fractions of the width of a diode, by either half- or quarter-diode widths, and then storing those as separate spectra in the onboard memory. These were merged into a single spectrum in the data reduction phase. The manner in which this was done was specified by the STEP-PATT parameter, described in more detail in Chapter 35 (see Table 35.3). The choice of STEP-PATT also determined how the background around the spectrum was measured. Figure 34.5 shows the diode arrangement; note the six large corner diodes and six focus diodes (numbers 4, 5, and 6, for example).

Figure 34.5: Diode Layout in the Digicon Detectors



34.2.3 Internal Calibration

The GHRIS was built with two Pt-Ne hollow-cathode lamps to provide a rich spectrum of emission lines for accurate calibration of wavelengths. The locations of these lamps and the way in which they illuminated the spectrograph optics are illustrated in the *GHRIS Instrument Handbook*. The apertures through which calibration exposures were made were the same size as the Small Size Aperture (SSA). Moreover, calibration aperture SC2, the one most frequently used, was offset from the SSA in the x direction (the direction of dispersion), but was aligned in the y direction (see Figure 34.1). This offset in x introduced a systematic shift in wavelength between the SSA and SC2 because light from them hit the gratings at different angles. By convention, the wavelength scale of the GHRIS was calculated so as to be correct for the SSA.

These wavelength calibration lamps were also used for other internal instrumental calibrations, such as DEFCALs (deflection calibration) and SPYBALs (Spectrum-Y-Balance). Only one of these lamps was available for use after the failure of Side 1 in 1991. A wavelength calibration exposure (WAVECAL) was obtained by specifying an ACCUM in the Phase II Proposal with a target of WAVE and an aperture of SC2. (Prior to 1991, SC1 was a valid aperture designation and so older observations may show it.)

A WAVECAL is not the only way to assess the quality of the wavelength scale for observations. As will be noted in the example for R136a, a SPYBAL was obtained just before an ACCUM that used a grating for the first time. A SPYBAL was just a WAVECAL that was obtained at a predetermined carousel position for each grating, and SPYBALs were done to align the spectrum on the diodes in the y direction (perpendicular to dispersion). A SPYBAL contains wavelength information that can be used to check for zero-point offset.

34.2.4 Side 1

The installation of the GHRIS Redundancy Kit during the first servicing mission (December 1993) eliminated the risk of a Side 1 power supply failure affecting Side 2. With this risk removed, Side 1 operations were resumed during Cycle 4. These operations were nominal.

When the Side 1 carousel was commanded through the Side 2 electronics during a Side 1 observation, the telemetry word containing the carousel position would read the Side 2 commanded position during carousel configuration, and the Side 1 encoder position after integration. The Side 1 GHRIS data headers do contain the correct Side 1 position of the carousel.

GHRIS Side 1 observations cover the time spans April 1990 to June 1991 and February 1994 to the Second Servicing Mission.

34.2.5 COSTAR

The spherical aberration of the HST primary mirror was corrected by the first servicing mission (December 1993) with the installation of the Corrective Optics

Space Telescope Axial Replacement (COSTAR) assembly. COSTAR deployed corrective reflecting optics in the optical path of the GHRS. The post-COSTAR GHRS has a different response with wavelength than the pre-COSTAR instrument. Interim sensitivity files were installed in CDBS on April 16, 1994, and updated during Cycle 4 and 5 when calibration observations became available. GHRS observations obtained early in Cycle 4 will require recalibration.¹

34.3 Operating Modes and Data Types

The GHRS had two principal science data acquisition modes: accumulation (ACCUM) and rapid readout (RAPID or DIRECT READOUT), as well as onboard target acquisition modes and a rudimentary image mode which was sometimes used to image the sky through the science aperture. We provide a high-level overview of these modes here, with more detail provided in Chapter 35.

34.3.1 Acquisitions and Images

Almost all GHRS visits began with an acquisition of an object. Most GHRS targets were point sources (i.e., stars), but there were also many observations of planets, nebulae, and galaxies. Almost all acquisitions were of the ONBOARD type, i.e., they were done autonomously by the GHRS. In a few cases, especially soon after launch, acquisitions were interactive. There are also some cases of “early acquisitions,” in which an image was first obtained with WF/PC, FOC, or WFPC2, well in advance of the GHRS observation.

IMAGE mode was used to create an image of the GHRS aperture being used. Obviously this would be a very small region of the sky, but it would be taken in the ultraviolet, and it would show how the light of the object was distributed in the aperture, which was sometimes helpful for after-the-fact analysis of what was observed. A similar mode was invoked if a MAP were requested. GHRS acquisitions are explained in “Understanding GHRS Acquisitions” on page 35-19.

34.3.2 ACCUMs

ACCUM mode was by far the most commonly used mode of the GHRS as it allowed the use of all the automatic procedures for optimizing the data acquisition (FP-SPLIT, substepping, and comb addition—see “Detectors” on page 34-7). The calibrated data (.c1h and .c0h files) for a typical ACCUM mode observation will have multiple groups. Each of these groups is an independent (sub)integration and they must be added together (realigning the data in wavelength space before adding) to produce the total calibrated spectrum for your observation. See

1. We recommend, as a rule, that archival researchers recalibrate *all* GHRS observations in order to take advantage of the best calibrations and knowledge that is available.

“Assessing GHRS Science Data” on page 35-29 for examples of ACCUM data and a description of how to reduce and analyze such data.

WSCAN was a variant of ACCUM in which one could specify a range of wavelengths to be observed and the software would determine how to space grating movements to accomplish that. OSCAN was another variant of ACCUM that applied only to the echelle gratings (scanning through orders); it was used almost exclusively for calibrations.

34.3.3 RAPID Mode

For observations of targets whose spectra varied on shorter timescales, there was *rapid* (or *direct*) readout mode. In RAPID mode, individual integrations could be obtained as often as once every 50 milliseconds. However, RAPID mode did not allow use of the FP-SPLIT or substepping procedures and observations of the detector background were not interspersed with the on-target observations. In RAPID mode data, each subintegration was stored sequentially in separate groups in both the raw and the calibrated data.

RAPID mode resulted in huge data quantities, and was used to search for forms of time variability. See “RAPID Mode (and a Little About Spatial Scans)” on page 35-34 for examples of RAPID mode data and a discussion of how to work with it.

34.4 Documentation and References

34.4.1 STScI GHRS Documentation

Many of the documents described in this section are available only as paper. Archival users should not generally need them, but if needed, copies are cataloged² and stored in the STScI Library.

Instrument Handbooks

The *GHRS Instrument Handbook* is the single most useful reference about the GHRS except for this data handbook; it describes instrument operating modes as well as observing strategies. The instrument handbook is critical for understanding why a series of observations may have been obtained in a particular manner at a particular time. The flight software and operating procedures for the GHRS changed continually over its life as errors were corrected and new features installed. The different versions of the instrument handbook document the history of these efforts (as do the ISRs, described below).

2. If you search the library’s on-line catalog for GHRS documents, try the string “HRS” because many older documents pre-date the addition of “Goddard” to the name.

Eight versions of the *GHRIS Instrument Handbook* were issued by STScI between October, 1985, and June, 1995. The first four versions (1.0, 2.0, 2.1, and 3.0) exist as paper-only documents, and they pertain to the pre-COSTAR instrument. The last four versions (4.0, 4.1, 5.0, and 6.0) are available on-line as Adobe Acrobat and world wide web documents, and were written for the post-COSTAR instrument.

The instrument handbook contains information pertinent to specific time periods and cycles of HST operation. Archival researchers should not need to refer to these documents but we list them in Table 34.2 for completeness.

Table 34.2: GHRIS Instrument Handbook Versions

IH version	Date of Issue	HST Cycle
2.0	May, 1989	1, 2
3.0	January, 1992	3
4.0	January, 1993	4
5.0	May, 1994	5
6.0	June, 1995	6

Instrument Science Reports

Instrument Science Reports (ISRs) are technical papers issued by STScI that summarize, for example, calibrations, or new operating features. Ninety-one GHRIS ISRs were written. Sometimes ISRs provide details not available elsewhere, but in general we have tried to encapsulate the contents of ISRs into this data handbook so that archival researchers will not need to refer to them. There are some cases where the ISR treats a specialized subject that is beyond the scope of this handbook, and we note those where appropriate.

34.4.2 GHRIS Web Resources

STScI maintains extensive resources on the World Wide Web. GHRIS resources can be found by using the search mechanism. You should always check there for changes or updates. STScI's home page is at:

<http://www.stsci.edu/>

34.4.3 GHRIS Bibliography

The following papers include discussions of GHRIS construction and performance or provide detailed explanations of particularly useful data analysis techniques. A more complete list of references is available on the web and as *GHRIS ISR 91*.

Primary Reference for GHRS Performance

The following paper should, in most cases, be cited when referring to GHRS observations:

- Heap, S.R., et al., “The Goddard High Resolution Spectrograph: In-Orbit Performance,” 1995, *PASP*, 107, 871.

Ultraviolet Reddening and Extinction

- Bless, R.C., and B.D. Savage, “Ultraviolet Photometry from the Orbiting Astronomical Observatory. II. Interstellar Extinction.” 1972, *ApJ*, 171, 293–308.
- Nandy, K., G.I. Thompson, C. Jamar, A. Monfils, and R. Wilson, “Studies of Ultraviolet Interstellar Extinction with the Sky-survey Telescope of the TD-1 Satellite.” 1976, *A&A*, 51, 63–69.
- Code, A.D., J. Davis, R.C. Bless, and R. Hanbury Brown, “Empirical Effective Temperatures and Bolometric Corrections for Early-Type Stars.” 1976, *ApJ*, 203, 417–434.
- Seaton, M.J., “Interstellar Extinction in the UV” 1979, *MNRAS*, 187, 73P–76P.
- Savage, B.D., and J.S. Mathis, “Observed Properties of Interstellar Dust” 1979, *ARA&A*, 17, 73–112.

GHRS-Related Technical Papers

- Ebbets, D.C., J.C. Brandt, and the HRS Investigation Definition Team, “Ultraviolet High-Resolution Spectroscopy from the Space Telescope,” 1983, *PASP*, 95, 543–549.
- Reader, J., N. Acquista, C.J. Sansonetti, and J.E. Sansonetti, “Wavelengths and Intensities of a Platinum/Neon Hollow Cathode Lamp in the Region 1100–4000 Å,” 1990, *ApJS*, 72, 831–866.
- Ebbets, D.C., J. Brandt, and S. Heap, S., “Status of the Goddard High Resolution Spectrograph in May 1991,” in *The First Year of HST Observations*, edited by A.L. Kinney and J.C. Blades, 1991, p. 110-122.
- Cardelli, J.A., D.C. Ebbets, and B.D. Savage, “Scattered Light in the Echelle Modes of the Goddard High Resolution Spectrograph Aboard the Hubble Space Telescope. I. Analysis of Prelaunch Calibration Data.” 1990, *ApJ*, 365, 789–802.
- Cardelli, J.A., D.C. Ebbets, and B.D. Savage, “Scattered Light in the Echelle Modes of the Goddard High Resolution Spectrograph Aboard the Hubble Space Telescope. II. Analysis of Inflight Spectroscopic Observations.” 1993, *ApJ*, 413, 401–415.
- Gilliland, R.L., S.L. Morris, R.J. Weymann, D.C. Ebbets, D.C., and D.J. Lindler, “Resolution and Noise Properties of the Goddard High Resolution Spectrograph,” 1992, *PASP*, 104, 367–382. (Discusses deconvolution of the effects of the GHRS PSF and LSF.)

- Brandt, J.C., et al., “The Goddard High Resolution Spectrograph: Instrument, Goals, and Science Results,” 1994, *PASP*, 106, 890–908. (Publication of record for the pre-COSTAR GHRS.)
- Blades, J.C., and S.J. Osmer, editors., *Calibrating Hubble Space Telescope: Proceedings of a Workshop Held at STScI* published by STScI. (Contains several papers of relevance for data analysis.)
- Lyu, C.-H., F.C. Bruhweiler, and A.M. Smith, “Tomography/Power Spectrum Techniques for Removal of Fixed Pattern Noise from Hubble Space Telescope Spectra,” 1995, *ApJ*, 447, 880–888.
- Lallement, R., J.-L. Bertaux, J.T. and Clarke, “Deceleration of Interstellar Hydrogen at the Heliospheric Interface” 1993, *Science*, 260, 1095–1098. (Provides a good illustration of geocoronal Ly- α with the LSA and Echelle-A.)
- Lambert, D.L., Y. Sheffer, R.L. Gilliland, and S.R. Federman, “Interstellar Carbon Monoxide toward ζ Ophiuchi,” 1994, *ApJ*, 420, 756–771. (Discusses how to achieve very high signal-to-noise with the GHRS.)

